NeuroImage: Clinical 31 (2021) 102761

Contents lists available at ScienceDirect

NeuroImage: Clinical

journal homepage: www.elsevier.com/locate/ynicl

Abnormal effective connectivity in the sensory network in writer's cramp

Inken Tödt [a,1,*], Alexander Baumann [a,1], Arne Knutzen [a], Oliver Granert [a], Elinor Tzvi [b], Julia Lindert [c], Stephan Wolff [d], Karsten Witt [e], Kirsten E. Zeuner [a]

[a] Department of Neurology, Kiel University, Germany
[b] Department of Neurology, Leipzig University, Germany
[c] Brighton and Sussex University Hospitals NHS Trust, UK
[d] Department of Radiology, Kiel University, Germany
[e] Department of Neurology and Research Center Neurosensory Science, School of Medicine and Health Sciences - European Medical School, Carl von Ossietzky University, Oldenburg, Germany

ARTICLE INFO

Keywords:
Dynamic causal modeling
fMRI
Focal hand dystonia
Writer's cramp
Network disorder
Sensory network

ABSTRACT

Background: Writer's cramp (WC), a task specific form of dystonia, is considered to be a motor network disorder, but abnormal sensory tactile processing has also been acknowledged. The sensory spatial discrimination threshold (SDT) can be determined with a spatial acuity test (JVP domes). In addition to increased SDT, patients with WC exhibited dysfunctional sensory processing in the sensory cortex, insula, basal ganglia and cerebellum in a functional magnetic resonance imaging (fMRI) study while performing the spatial acuity test.
Objectives: To assess whether effective connectivity (EC) in the sensory network including cortical, basal ganglia, thalamic and cerebellar regions of interest in WC patients is abnormal.
Methods: We used fMRI and applied a block design, while 19 WC patients and 13 age-matched healthy controls performed a spatial discrimination task. Before we assessed EC using dynamic causal modelling, we compared three model structures based on the current literature. We enclosed regions of interest that are established for sensory processing during right hand stimulation: Left thalamus, somatosensory, parietal and insular cortex, posterior putamen, and right cerebellum.
Results: The EC analysis revealed task-dependent decreased unidirectional connectivity between the insula and the posterior putamen. The connectivity involving the primary sensory cortex, parietal cortex and cerebellum were not abnormal in WC. The two groups showed no differences in their behavioural data.
Conclusions: Perception and integration of sensory information requires the exchange of information between the insula cortex and the putamen, a sensory process that was disturbed in WC patients.

1. Introduction

Although the main symptoms of writer s cramp (WC) point to an impaired motor function, sensory dysfunction has been identified as a fundamental characteristic of several types of adult-onset focal dystonia (Avanzino et al., 2015; Conte et al., 2019; Quartarone and Hallett, 2013). Patients with WC revealed abnormal proprioceptive (Kaji et al., 1995; Trompetto et al., 2006), nociceptive (Suttrup et al., 2011) and tactile information processing. Specifically, increased temporal (Conte et al., 2014; Fiorio et al., 2003; Sanger et al., 2001) and spatial discrimination thresholds (SDT) (Bara-Jimenez et al., 2000a; Molloy et al., 2003; Sanger et al., 2001) have been reported previously.

Beyond a deficient sensory system, dystonia is considered as a sensorimotor network disorder that includes multiple dysfunctional cortical and subcortical areas (Hanekamp and Simonyan, 2020; Lacruz et al., 1991; Neychev et al., 2011; Rothkirch et al., 2018; Simonyan, 2018). Structural and functional imaging has been applied to understand the underlying pathophysiology. Using voxel based morphometry increases (Garraux et al., 2004) as well as decreases (Delmaire et al., 2007) of grey matter volume in the primary somatosensory cortex were detected in dystonia. Additionally, functional connectivity was strengthened between the somatosensory cortical-putamen loop during a visuo-motor control task in WC (Moore et al., 2012). The putamen itself had elevated grey matter volume in patients with task specific

* Corresponding author at: Department of Neurology, Kiel University, Arnold-Heller-Str. 3, Haus D, 24105 Kiel, Germany.
E-mail address: i.toedt@neurologie.uni-kiel.de (I. Tödt).
[1] Shared first authorship.

https://doi.org/10.1016/j.nicl.2021.102761
Received 19 April 2021; Received in revised form 7 July 2021; Accepted 8 July 2021
Available online 15 July 2021

dystonia (Granert et al., 2011; Zeuner et al., 2015). Its posterior part is involved in sensory processing (Alloway et al., 2017; Reig and Silberberg, 2014). The thalamus is another well-known region contributing to sensory processing. In patients with WC, grey matter decreases were found in the thalamus bilaterally (Delmaire et al., 2007). This area is considered as a central dysfunctional hub integrating basal ganglia and cerebellar output and gating sensory streams (Conte et al., 2019).

In patients with cervical dystonia, decreased connectivity between the basal ganglia and the cerebellum has been reported (Filip et al., 2017). Their importance for the motor system and the sensory function of the basal ganglia are established. More previously sensory cerebellar activation has been identified as well (Wiestler et al., 2011). The cerebellum is activated during temporal and spatial discrimination (Maria A. Pastor et al., 2004). Structural alterations (Delmaire et al., 2007) as well as abnormal cerebello-cortical (Dresel et al., 2014) and cerebello-putaminal connectivity (Moore et al., 2012) have been described in dystonic patients, while they seem to improve their handwriting after cerebellar electrical transcranial stimulation (Bradnam et al., 2015). Finally, the parietal cortex is considered to be crucial for multisensory integration (Avanzino et al., 2015), and in patients with WC reduced functional connectivity between parietal and motor areas has been observed (Delnooz et al., 2012). Although sensory abnormalities are widely accepted, the interactions within the network remain speculative. Thus, this study was designed to investigate effective connectivity or the directed influence one region has over another (Friston, 2009) using dynamic causal modelling (DCM) in patients with WC performing a sensory paradigm during fMRI. We chose a spatial acuity task (Van Boven and Johnson, 1994), as patients with WC showed abnormal sensory processing (Bara-Jimenez et al., 2000b) and deficient activation in several areas of the sensory network (Peller et al., 2006).

We hypothesized that the relative degree of effective connectivity within the sensory network would differ between WC patients and a healthy control group. In particular, we expected abnormal cortical sensory processing in the primary somatosensory cortex, that interferes with the posterior putamen and the thalamus, because these areas are important for sensory processing such as tactile discrimination (Lacruz et al., 1991). The insula was also included, because the somatosensory cortex is linked to the insula and the posterior striatum (Lehéricy et al., 2004). Further, we explored possible abnormalities of uni- or bidirectional effective connectivity between the cerebello- parietal cortical and cerebello- thalamo-striatal loop. Our analysis is based on two network models: the first one postulates faulty thalamic gating of sensory information. The thalamus is considered a central dysfunctional hub and is responsible for processing sensory information from the cerebellum and the basal ganglia. The result is an abnormally elevated input and dysfunction of somatosensory cortical areas (Conte et al., 2019). The second model, derived from the work of Avanzino et al. (Avanzino et al., 2015), is also based on subcortical sensory input from the same structures including the thalamus and cerebellum that is further directed to the basal ganglia and premotor cortex. The basal ganglia are bidirectional connected to the somatosensory cortex, which further projects to the parietal cortex and the motor cortex. Dystonia might result from deficits in sensory-motor integration and from dysfunctions at different levels of this network.

2. Methods

2.1. Subjects

In the DCM analysis we included 19 right-handed (laterality quotient 89.1 ± 10.1) according to the Edinburgh Handedness Inventory (Oldfield, 1971) WC patients (10 male). 8 patients presented with simple WC with only writing being affected, while in 11 patients additional fine motor tasks other than writing were impaired (complex WC). Here, we were very strict in the definition of simple versus complex writer's cramp that is that patients who had one more task affected by dystonic co-contraction were considered as complex writer's cramp. All patients clearly had dystonia only when targeting the task specific element. None of them had dystonic co-contraction when not performing that specific task. The diagnosis of WC was established by medical history and standard neurological examination including a writing test of the affected hand (Table 1).

We included 13 (5 male) right-handed (laterality quotient 88.7 ± 9.3) (Oldfield, 1971), age-matched healthy controls (HC) (age 53.54 ± 8.03 years). The groups were equally distributed according to age ($p = 0.91$) using a *t*-test for independent groups and gender ($p = 0.49$) using a Fisher's exact test. Exclusion criteria included i.) neurological or psychiatric disorders other than WC, ii.) peripheral neuropathy of the median nerve and iii.) inability to recognize the orientation of the 3.0 mm dome. Written informed consent was obtained from all participants. The study was approved by the Ethics Committee of the Medical Faculty of the University of Kiel and was conducted in full accordance with the declaration of Helsinki.

2.2. Experimental design

2.2.1. Sensory procssing paradigm: fMRI

Prior to scanning we performed the grating orientation task (GOT) with the JVP domes (Van Boven and Johnson, 1994) in every subject to measure the SDT. The JVP domes are small, round stamps with grooves of different widths cut into the surfaces. Each dome was pressed twenty times for one second each in either horizontal or vertical direction on the tip of the index finger. The subject had to differentiate between these two orientations. We started with the dome of greatest width (3.0 mm) and continued with 2.0, 1.5, 1.2, 1.0, 0.75, 0.5- and 0.35-mm domes. The gap value at which the participant recognized 75% of the orientations correctly was considered as the SDT.

During fMRI the subject‘s right hand was positioned in a supine position and a response button was placed in the left hand. In the scanner, we only presented the 3 mm and the 0.35 mm domes in a pseudo-randomized order. While the horizontal and vertical direction of the 3 mm dome could be identified by every subject, the latter one was perceived as smooth and served as a control condition (Peller et al., 2006). Each fMRI block consisted of two alternating 25 sec epochs of rest and task. Following 5 sec of visually presented instructions, the dome was applied 5 times for 5 sec in the same direction. The subject had to discriminate between three conditions horizontal (3 mm), vertical (3 mm) and smooth (0.35 mm). For indicating the perceived orientation, the subject had 5 sec to push one of three possible buttons with the left hand (Fig. 1).

2.2.2. Image acquisition and processing

Anatomical and functional images were acquired with a 3.0 T whole-body MRI scanner (Achieva; Philips, Best, the Netherlands) with a 32-channel head coil. An Invivo IFIS fMRI system (Invivo, Gainesville, Florida, USA) was used for stimulus presentation. For fMRI, the first three scans of each session were discarded due to non-equilibrium of magnetization, followed by 300 echo planar images with 38 ascending transversal slices (Field of view = 215x215x215mm^3, voxel size = 3.37 × 3.37 × 3.30 mm^3, slice thickness = 3.0, gap = 0.3, TR = 2500 ms, TE = 36.4 ms, flip angle = 90). For spatial normalization and exclusion of gross structural abnormalities, a 3D T1-weighted image was acquired (scan duration = 282 sec, slices = 160 sagittal, slice thickness = 1, field of view = 240x240x160mm^3, voxel size = 0.94 × 0.94 × 1 mm^3, TR = 7.749 ms, TE = 3.6 ms, flip angle = 8.0).

Pre-processing and analysis of the fMRI data and DCM analysis were performed with SPM 12 (SPM12; Welcome Department of Imaging Neuroscience, London, http://www.fil.ion.ucl.ac.uk) executed in MATLAB Version 9.3 (R2017b) (MathWorks Inc., Natick, Massachusetts, USA). For a detailed description of the pre-processing steps and parameters, please see Rothkirch et al. (2018). Images were smoothed using a Gaussian kernel filter of 9 mm full-width at half-maximum

Table 1
Characteristics of included patients with writer's cramp.

Patient ID	Age (ys)	Sex	Symptom Duration (ys)	Type of WC	Duration BoNT treatment (ys)	Last injection (months)	Total ADDS score (%)	WCRS score
P101	69	f	9	complex	8	4	60.00	10
P103	52	f	7	simple	0.25	14	72.85	6
P108	36	f	11	simple	NA	NA	55.71	8
P110	60	m	14	simple	NA	NA	51.43	6
P111	39	f	12	simple	NA	NA	55.71	17
P113	54	m	6	complex	NA	NA	51.43	5
P114	53	m	14	complex	0.25	36	55.71	5
P115	56	m	14	simple	10	5	60.00	10
P117	70	f	15	complex	NA	NA	68.57	13
P119	35	m	21	complex	0.5	36	48.85	14
P123	68	f	25	complex	0.5	132	25.71	8
P124	50	m	17	complex	3	96	42.85	8
P125	55	f	4	complex	3	18	81.43	5
P126	45	m	30	complex	3.5	3	68.57	5
P128	57	m	34	complex	2	10	34.29	12
P130	60	m	7	simple	0.25	60	77.14	3
P131	29	f	1	simple	NA	NA	68.57	11
P132	78	f	6	complex	3	4	68.57	5
P133	24	m	1	simple	NA	NA	68.57	11
Mean ± SD	52 ± 15		13 ± 9				62.57 ± 13.04	8.53 ± 3.68

Legend: ADDS: Arm Dystonia Disability Scale; BoNT: botulinum neurotoxin; f: female, m: male; NA: not applicable (patients without BoNT treatment); WCRS: Writer's Cramp Rating Scale; ys: years.

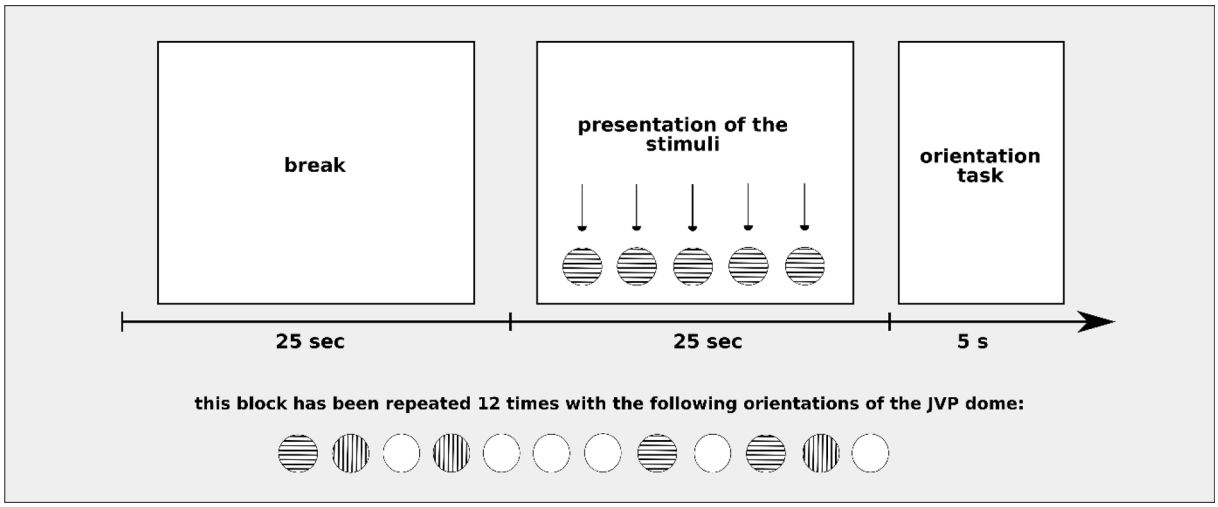

Fig. 1. fMRI paradigm of the SDT task with the timing of one block (upper panel) and pseudo-randomized order of the 3.00 mm and 0.35 mm dome orientation (lower panel).

(FWHM) as our normalization wrote $3 \times 3 \times 3$ mm^3 EPI images.

The first level analysis of the sensory task was modelled as a block design using a General linear model (GLM) with two regressors of interest: The *sensory* regressor, accumulates all stimuli blocks with the 3.00 mm domes independent from their orientation and the second *smooth* regressor captures all blocks with the finer 0.35 mm domes. As regressors of no interest the six realignment parameters were included. On the second (group) level, we used separate SPM models to compute the main effect of conditions per group (HC, WC) by means of a one sample t-tests with the respective first level contrast images. Group differences (HC vs. WC) were assessed by two sample t-tests for all conditions. To reduce the variance of the BOLD signal, results of behavioural data (Fahn Score, Wissel score, disease duration, age, tactile thresholds and correct spatial discrimination of orientation) were used as covariates in a separate analysis.

2.3. Dynamic causal modeling

2.3.1. Specifying plausible model structures of endogenous and exogenous connectivity

For the specification of different model structures, we included 5 regions of interest (ROI) known to be involved in the processing of sensory stimuli of the right hand: Left thalamus, right cerebellum crus I, left somatosensory cortex, left posterior putamen and the left parietal cortex. As a result of our second level analysis, we included the left insula as ROI. Based on these ROIs, we specified different model structures according to the current literature. **Model 1** is derived by the synopsis of our current understanding of the sensory network of focal dystonia. This model reflects the interaction between sensory cortical areas, the cerebellum and a central subcortical hub including the thalamus and the posterior putamen. Although this analysis is dealing with effective connectivity, all direct connections were checked and adjusted according to anatomic substrates (Bostan and Strick, 2018; Caligiore et al., 2017; Ghaziri et al., 2018; Lanciego et al., 2012; Milardi et al., 2019; Ramnani, 2012).

Model 2 is based on the review of Conte and colleagues about altered

sensorimotor processing in focal dystonia (Conte et al., 2019). For **Model 3** we referred to the review of Avanzino et al. (2015). We adapted the models of Conte and Avanzino to the included ROIs discussed above and excluded the motor areas such as the motor cortex and the pontine areas, because a model comparison with DCM is limited to models with the same model space.

2.3.2. Regions of interest (ROIs)

To extract time series from significant voxels in each region of interest (ROI) in the *sensory* contrast, we masked the statistical map of individual first level analysis with an anatomical automated labelling (AAL) mask of the respective area defined previously. Subject-specific sphere centres were defined as the nearest suprathreshold voxel to the main effect of the *sensory* contrast over all participants within this masked area ($P < 0.05$). The sensory contrast is based on the 25 sec of index finger stimulation contrasted to baseline activation (see Fig. 1). The individual time series were then computed as the first eigenvariate across all suprathreshold voxels within 6 mm (somatosensory cortex, insula and parietal cortex) or 4 mm (thalamus, posterior putamen) radius from the individual sphere centre and adjusted for effects of no interest (movement parameters). We chose different sphere sizes to reflect the anatomical dimension of the respective areas. The parameters (4 mm or 6 mm spheres) were selected in accordance to previous DCM research performed in this field (Pool et al., 2013; Tzvi et al., 2015). The purpose was to account for the different dimensions of the anatomical structures included as ROIs. To ensure that the individual sphere centres are located adjacent to the predefined sphere centres, we calculated the Euclidean distance between them. A distance greater than 10 mm was not accepted. The mean Euclidian distances between the predefined and the individual sphere centres were the following: Thalamus = 3.02 ± 3.22, S1 = 1.62 ± 1.38, cerebellum = 1.33 ± 2.18, posterior putamen = 5.13 ± 4.40, insula = 5.47 ± 3.04, PC = 1.94 ± 2.59 (all distances given in mm). A careful selection of the included subjects by means of the strict adherence to the predefined thresholds and controlling for a homogenous location of ROIs is important for a valid DCM analysis and therefore its interpretation. Along our predefined exclusion criteria, we could include 19 patients and 13 healthy controls out of a pool of 33 WC patients and 36 HC.

2.3.3. Bayesian model selection and parameter averaging

After estimating each of the three predefined models for all subjects we conducted a Bayesian Model Selection (BMS) as an established statistical procedure based on the computation of an approximation to the model evidence p(y|m). This probability gives information about how likely the measured data y is under the assumption of a certain model m. For our data we chose a random effects analysis (RFX) BMS, which does not, in contrast to a fixed effects analysis, assume an identical optimal model structure in the population and is therefore more robust against outliers (Stephan et al., 2010). When performing RFX BMS the recommendation is to use family-level inference, because RFX BMS results may possibly be incorrect (Penny et al., 2010). The model with the highest model evidence per group is referred to as the winning model. After estimating the winning model in each group, we averaged the model parameters and computed Wilcoxon-signed rank tests on group level, adjusted for alpha inflation (False discovery rate (FDR) corrected) within each connectivity matrix (model matrices A and B) and group (WC and HC) to test whether the averaged parameters differed significantly from zero and then compared the corresponding parameters between the groups to identify potential group differences.

3. Results

3.1. Behavioural results of the tactile discrimination task

Before scanning, the SDT were assessed for left and right index finger and showed no difference between the groups using the Wilcoxon rank sum test (left finger: $Median_{WC} = 2.44$; $Median_{HC} = 1.5$; $W = 166.5$, $p = 0.1$; right finger: $Median_{WC} = 2.33$; $Median_{HC} = 2.4$; $W = 116.5$, $p = 0.80$). Within the MRI the average number of correct answers for the 3.0 mm dome was similar between the groups ($Median_{WC} = 11$, $Median_{HC} = 12$, $W = 93$, $p = 0.22$). This means that there were no differences in sensory discrimination between WC patients and healthy controls.

3.2. Functional imaging results

As main effect of the *sensory* condition, all subjects exhibited increased BOLD signal in a widespread network of the bilateral precentral and parietal gyrus, bilateral cerebellum lobule VI, bilateral thalamus, bilateral pallidum and further areas corrected for multiple comparisons (Table 2).

Additionally, for the contrast *sensory* the WC group showed significant increased BOLD signal compared to controls in the left insula ([xyz] = [−30, 8, 8], t (67) = 4.65, $p \leq 0.05$, FWE corrected). There were no changes within the statistical parametric maps after adding covariates (age, Fahn Score etc.) to the model on the second level.

3.3. Dynamic causal modelling analysis

3.3.1. Bayesian model selection

Using RFX BMS, the model reflecting the sensory network model postulated by Conte et al. (2019) extended by the parietal cortex and the insula (Model 2, Fig. 2) showed the highest expected posterior probability (exp_r) in both groups (HC: $exp\_r_{Mod1} = 0.0619$, $exp\_r_{Mod2} = 0.8754$, $exp\_r_{Mod3} = 0.0628$; WC: $exp\_r_{Mod1} = 0.0447$, $exp\_r_{Mod2} = 0.8638$, $exp\_r_{Mod3} = 0.0915$). This led us to conclude that this model is most likely the generative model of the given data. Further results of the RFX BMS procedure can be seen in Fig. 2.

To ensure model inversion and validity, we tested for the winning model on a single subject level the determination coefficient and the strength of model parameters. The percent of explained variance should be greater than 10% and one of the model parameters should have a strength of 1/8 Hz or more. The mean variance explained was 37.9 ± 4.7 % in the WC and 37.7 ± 6.9 % in the HC group with the percent variance explaining greater than 28.06 % for all patients' and HC models. We were able to include all connections, because the parameter estimates were higher than 1/8 Hz. For the timeseries extraction, we chose relatively liberal thresholds. Therefore, we checked the explained variance of those VOIs. In all subjects, the explained variance was greater than 67.88 % in all ROIs (minimal variance explained: Thalamus: 76.9 %; Insula: 76.9%; S1: 80.9%; Cerebellum: 81.3%; Putamen: 67.9%; Parietal Cortex: 76.2%).

Table 3 displays the group- wise averaged connectivity parameters for the intrinsic (matrix A) and Table 4 the task- dependent connectivity (matrix B) between the regions of the winning model. A connectivity parameter is considered significant with a value below 0.05 after FDR correction for multiple comparisons (corrected separated for groups and matrices). For the intrinsic connectivity (Table 3), reflecting the effects that the afferents within the model exerts on the dynamics of the system, we found no differences between WC and HC.

The modulatory effect of the 3.00 mm domes on connectivity was positive and reached significance in all connections (B matrix, Table 4, Fig. 3) in WC as well as in HC (Table 4). A significant group difference in the effective connectivity was found in the insula- putaminal connection with a less strong connectivity in the WC group.

4. Discussion

To our knowledge this is the first study using DCM to assess effective connectivity in an exclusively sensory network in patients with WC performing a spatial acuity task. There are three main findings: First, WC patients demonstrated an increased BOLD signal in the left insula compared to controls. Second, the winning model was the model for

Table 2
Main effect of tactile discrimination task of the 3 mm dome corrected for multiple comparisons ($p \leq 0.05$, FWE corrected).

	MNI coordinates Left hemisphere				MNI coordinates Right hemisphere			
AAL label	x	y	z	t-value	x	y	z	t-value
Precentral	−33	−7	62	11.23	36	−7	56	11.40
Parietal_Inf	−45	−34	41	16.16	42	−46	44	14.43
Insula	−30	23	5	12.70	39	2	5	8.39
	−39	−1	11	12.35				
Thalamus	−12	−13	2	6.3	15	−10	2	5.56
Pallidum	−24	−1	−1	9.46	21	8	3	6.56
Supp_Motor_Area					6	11	50	14.27
Frontal_Mid	−33	38	23	7.01	33	35	23	11.61
Cerebellum_crus_6	−27	−61	−28	9.78	24	−55	−25	11.25

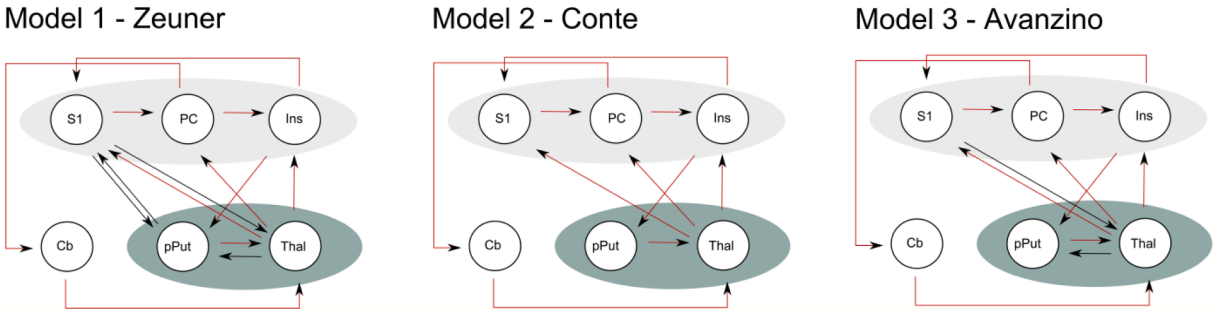

Fig. 2. Three plausible model structures for Bayesian model selection in DCM. The cortical cluster (grey background) contains the primary somatosensory cortex (S1), the parietal cortex (PC) and the insula (Ins), the subcortical cluster (green background) contains the posterior putamen (pPut) and the thalamus (Thal). The cerebellum (Cb) serves as an independent modulator. Red lines show connections that are identical across all three models. (For interpretation of the references to colour in this figure legend, the reader is referred to the web version of this article.)

Table 3
Task invariant (A-matrix) coupling parameters of the winning model in 1/s of the group- wise averaged DCMs within each group and differences in connectivity parameters between patients and controls ($p < 0.05$, FDR corrected separated by matrices and groups). The difference contrast was defined as $parameter_{HC} - parameter_{WC}$. A significant parameter greater than zero indicates a less strong influence of the connection in the patients' model, a significant parameter less than zero a stronger influence of the connection in the patients' model.

	WC (n = 19)		HC (n = 13)		Group differences
Connection	Parameter	p value	Parameter	p value	p value
Cb → Thal	0.2086	< 0.001#	0.1295	< 0.001#	0.3212
Put → Thal	0.1142	< 0.001#	0.2489	< 0.001#	0.1418
Thal → Ins	0.1536	< 0.001#	0.2303	< 0.001#	0.3579
PC → Ins	0.1585	< 0.001#	0.1995	< 0.001#	0.7601
Thal → S1	0.0770	< 0.001#	0.0993	0.0017#	0.3579
Ins → S1	0.0947	< 0.001#	0.1350	< 0.001#	0.3579
PC → Cb	0.2405	< 0.001#	0.1878	< 0.001#	0.3579
Ins → Put	0.2076	< 0.001#	0.3887	< 0.001#	0.1521
Thal → PC	0.2330	< 0.001#	0.2164	< 0.001#	0.7329
S1 → PC	0.1889	< 0.001#	0.2274	< 0.001#	0.8270

Legend: Cb: cerebellum, Ins: Insula, PC: parietal cortex, pPut: posterior putamen, S1: primary somatosensory cortex, Thal: thalamus.
Significant p value after FDR corrected at an overall p level ≤ 0.05.

Table 4
Task dependent (B-matrix) coupling parameters of the winning model in 1/s of the averaged DCMs ($P < 0.05$, Bonferroni corrected) within each group and differences in connectivity parameters between patients and controls ($P < 0.05$, Bonferroni corrected separated by matrices and groups). The difference contrast was defined as $parameter_{HC} - parameter_{WC}$. A significant parameter greater than zero indicates a less strong influence of the connection in the patients' model. A significant parameter smaller than zero indicates a stronger influence of the connection in the patients' model.

	WC (n = 19)		HC (n = 13)		Group differences
Connection	Parameter	p value	Parameter	p value	p value
Cb → Thal	0.1859	< 0.001#	0.1218	< 0.001#	0.4388
Put → Thal	0.0918	< 0.001#	0.1864	< 0.001#	0.132
Thal → Ins	0.0977	< 0.001#	0.1787	< 0.001#	0.2401
PC → Ins	0.1138	< 0.001#	0.1631	< 0.001#	0.5529
Thal → S1	0.0494	0.0012#	0.1062	0.0012#	0.1521
Ins → S1	0.0721	< 0.001#	0.1549	0.0002#	0.1629
PC → Cb	0.1138	< 0.001#	0.1547	0.0031#	0.5056
Ins → Put	0.1412	< 0.001#	0.3363	< 0.001#	0.0192#
Thal → PC	0.1693	< 0.001#	0.1944	< 0.001#	0.7876
S1 → PC	0.1377	< 0.001#	0.2095	< 0.001#	0.4177

Significant p value after FDR corrected at an overall p level ≤ 0.05.

altered sensorimotor processing suggested by Conte et al (Conte et al., 2019). Third, our imaging data showed a significant lower effective connectivity in WC patients in the insula-putaminal pathway. Since the

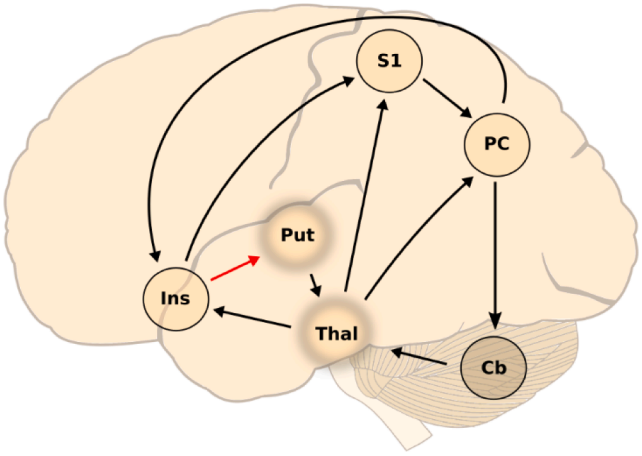

Fig. 3. Results of the dynamic causal modelling analysis on the basis of model 2. Black arrows indicate a significant influence of the sensory input on the connectivity between the respective regions in WC. The connection indicated in red reflects a less strong influence one region exerts over the other in WC compared to HC. Legend: Cb: cerebellum, Ins: Insula, PC: parietal cortex, pPut: posterior putamen, S1: primary somatosensory cortex, Thal: thalamus. (For interpretation of the references to colour in this figure legend, the reader is referred to the web version of this article.)

behavioural data showed no group differences these results indicate group specific BOLD signal changes. Thus, the abnormalities in connectivity between insula and putamen in WC patients have to be attributed to focal hand dystonia itself rather than to different sensory input.

4.1. Differences in BOLD signal during sensory discrimination

As a main result of fMRI analysis patients with WC revealed increased BOLD signal in the left insula. The insula is essential for the perception of touch (Preusser et al., 2015) and its activation during tactile discrimination has been described (Kitada et al., 2005; Peller et al., 2006). In a resting state fMRI analysis, enhanced functional connectivity was found between left thalamus and left S2/insula that correlated with disease activity in WC patients (Dresel et al., 2014). It is conceivable that the increase in BOLD signal is a correlate of pathological or compensatory sensory processing.

4.2. The winning model

It is most interesting that the model from Conte et al. was the winning model. There are some distinctive features that should be emphasized. Sensory input is processed to subcortical areas including the thalamus and the cerebellum and project to the to the sensory cortex, the parietal cortex and the insula. This approach is the same in all models. However, the model from Conte et al. contains the fewest degrees of freedoms, while the two alternative models showed bidirectional connections from the sensory cortex to the thalamus and between the thalamus and the basal ganglia. Conte et al point out that the thalamus plays a crucial role as it controls the sensory information to and from the cortex and is responsible for integrating sensory information within the basal ganglia and the cerebellum. Contrary to our expectations we were not able to find differences in effective connectivity between the groups between the thalamus and the sensory or parietal cortex.

4.3. Changes in effective connectivity

In this study, patients with WC demonstrated significantly weaker task-dependant unidirectional effective connectivity between the insula and the posterior putamen, while task independent connectivity was similar in both groups.

As mentioned already, the insula seems to play a major role in the perception of touch. Task dependent decreased effective connectivity from the insula to the posterior putamen reflects a problem in integrating and processing sensory input. Alternatively, it is conceivable that the increased activity in the insula causes a compensatory down-regulation of effective connectivity between insula and putamen. Our results are in accordance with the loss of insular hub in WC structural connectomes (Battistella et al., 2017; Hanekamp and Simonyan, 2020). The authors attributed their finding either to an abnormally enhanced internal representation of intended movements (Battistella et al., 2017) or a deficit of information coordination between areas that are involved in sensorimotor processing during movement planning (Hanekamp and Simonyan, 2020). However, contrary to our study they included motor areas such as the sensorimotor cortex and the anterior cingulate cortex, which were not part of our model since we concentrated only on the sensory system. Perception of touch requires the exchange of information between the insula cortex and the putamen (Preusser et al., 2015).

The putamen is important not only for motor processing (Rothkirch et al., 2018), but plays a major role for multimodal sensory integration. For example activation in the putamen correlated with the capability of healthy individuals to differentiate between one or two stimuli in a fMRI study (Pastor et al., 2008). Furthermore, putaminal enlargement has been described in patients with focal dystonia previously in several different studies (Granert et al., 2011, Conte et al., 2017). Patients with primary torsion dystonia (Bradley et al., 2009) and their unaffected relatives displayed abnormal temporal discrimination that was combined with a greater bilateral putaminal grey matter volume in a voxel based morphometry study. Thus, the abnormalities we noticed might reflect impaired sensory processing in the posterior putamen leading to a decreased communication between the putamen and the insula. However, we have to keep in mind that we only investigated the connection from the insular cortex to the putamen and not vice versa. Therefore, this remains speculative and it is unclear whether this is a primary phenomenon or a compensatory dysfunction.

Dystonia is considered a network disorder with defective communication between the basal ganglia, the cerebellum and the cortex. In contrast to our hypothesis, we were unable to detect differences in sensory processing from and to the cerebellum and the sensory cortex. Both, patients and controls demonstrated a task dependent connectivity from the somatosensory cortex to the posterior putamen and from the thalamus to the somatosensory cortex without any group disparities. We have to conclude from our data that in the grating orientation task used here sensory information processing in WC demonstrate a significant diminished EC between the left insular cortex and the left putamen, in the absence of any further EC changes in the somatosensory network.

The lack of a significant group specific effect in cerebellar connectivity in our study could be explained by the nature of the task. In the spatial discrimination task, the domes were passively presented to the index finger activating a haptic object recognition pathway that includes the somato-afferent fibres to the thalamus and further on to the somatosensory cortex. The decoding of tactile spatial information and the integration of these information into perceptual memory may be achieved by fronto-parietal areas (de Haan and Dijkerman, 2020). Cerebellar contributions are essential in action-related somatosensory processing. In this processing route the cerebellum receives input from the somato-sensory system and operates closely with the motor system whenever action and perception act in close relationship. Action-related somatosensory processing is a hallmark of writing. In the present study we focus on haptic object recognition demonstrating impaired connectivity on the level of the insula and the putamen. Further studies should integrate action-related somatosensory processing particularly to investigate the cerebellar contribution to dysfunctional connectivity in WC. For us, the finding that the connectivity to the somato-sensory cortex remained unchanged in the WC patients was unexpected. In WC, the cortical somato-sensory representation of fingers is abnormal.

The receptive fields of digits overlap. In the motor cortex of WC patients, a similar phenomenon has been described as a decrease of surrounding inhibition – a GABAergic intra-cortical system that sharpens focal and precise movements via lateral inhibition (Gallea et al., 2017). A failure of surrounding inhibition in WC patients lead to motor overflow and unwanted muscle spasms (Gallea et al., 2017). In a DCM analysis of the motor system in WC patients we found impaired functional connectivity in the basal ganglia and the cerebellar system directly involving M1 (Rothkirch et al., 2018). In the present study we focus on the sensory system. Here, we are not able to show the dysfunctional connectivity in cortical-subcortical communication in the sensory system that had been demonstrated in the motor system of WC patients.

4.4. Limitations

Against our expectations and the majority of the literature, we were not able to confirm the sensory deficit in our behavioural data. In our opinion, this has to be attributed to the unusual high threshold of our healthy controls. However, all participants were able to recognize the orientation of the 3.0 mm. Nevertheless, we detected significant changes in the cerebral dynamics during passive touching in the WC group and found profound changes in cerebral network dynamics. Given the fact that WC is characterized by the deficit of sensory-motor integration (Avanzino et al., 2015), we interpret our findings as a maladaptive processing of sensory integration as one part of deficit in sensory-motor integration which leads to the clinical phenotype of a motor disorder. Although, writer's cramp patients showed impaired perception and integration of sensory information, it remains unclear, whether this is a static trait or is dynamically linked to the occurrence of WC.

Another possible limitation could be that some patients were treated with botulinum toxin in the past. There are reports about the influence of botulinum toxin (BoNT) on the sensory system (Berardelli and Conte, 2021). However, most of the neurophysiological or neuroimaging studies that addressed the central effects of BoNT included patients with cervical dystonia (Berardelli and Conte, 2021; Khosravani et al., 2020). The measurements in these studies were performed just before BoNT treatment and four weeks later. One study measured spatial discrimination threshold in cervical dystonia and found an improvement of 23 % (Walsh and Hutchinson, 2007), but others reported contradictory results (Berardelli and Conte, 2021; Scontrini et al., 2011). The usual BoNT interval in the majority of studies is that there should be an interval after the last injection of at least three months. In our study only one patient had an interval of three and two patients of four months. All other patients had longer intervals for months or years or were never injected. Therefore, we do not think that BoNT had any influence on the effective connectivity in our study.

One aspect, that has to be discussed, is the methodical strictness we applied in the selection of the subjects included in the DCM analysis. As to our knowledge this was the first time, using DCM to investigate sensory processing in WC, we compared three possible literature-based DCMs and draw inference only on parameter space of the winning model. The thalamus has a powerful position in gating of somatosensory information and sensory-motor processing in cortico-subcortical loops, Therefore, it was included to the DCM analysis. This decision presupposes, however, that we have a valid BOLD signal within a circumscribed area of the thalamus. This was only feasible by excluding a relatively high amount of HC and making sure, that we have a high data quality within the included individuals in terms of a high amount of explained variance of the signal within the thalamus. Nevertheless, it cannot be excluded that there is a bias in the results due to the high exclusion of healthy controls. One restriction for the interpretation of the model structure derives from the definition of the model space. As dynamic causal modelling is a hypothesis-driven approach (Stephan et al., 2010), the model space is defined by specifying several plausible models. Given the diverse possibility for connections of the sensory network in humans, it is quite likely that we have not found the best model to explain the given data. Therefore, future research should include more or different relevant sensory regions.

Another limitation results from the definition of the regions of interest. As the choice of ROIs' extent and form are arbitrary, one can find different specifications. The here chosen parameters (4 mm or 6 mm spheres) are inspired by other DCM research done in this field (Pool et al., 2013; Tzvi et al., 2015).

5. Conclusion

In conclusion DCM analysis in patients with WC while performing a sensory spatial discrimination paradigm provides evidence for an abnormal sensory insula-striatal effective connectivity within the key nodes of the somatosensory network. The results underline the dysfunction of connectivity on the level of the basal ganglia most prominent in the posterior part of the putamen, whereas the functional network connectivity of the cortex and the cerebellums remain mainly intact. Our results underline the putamen as a dysfunctional node within the sensory system that may play a key role in the integration of sensorimotor integration in WC.

CRediT authorship contribution statement

Inken Tödt: Conceptualization, Methodology, Formal analysis, Writing - original draft, Visualization. **Alexander Baumann:** Conceptualization, Methodology, Formal analysis, Writing - original draft, Visualization. **Arne Knutzen:** Conceptualization, Methodology, Investigation, Project administration, Resources, Writing - review & editing. **Oliver Granert:** Software, Formal analysis, Resources, Writing - review & editing. **Elinor Tzvi:** Supervision, Validation, Writing - review & editing. **Julia Lindert:** Investigation, Resources, Writing - review & editing. **Stephan Wolff:** Resources, Investigation, Software. **Karsten Witt:** Conceptualization, Methodology, Validation, Funding acquisition, Supervision, Writing - review & editing, Visualization. **Kirsten E. Zeuner:** Conceptualization, Methodology, Project administration, Investigation, Resources, Funding acquisition, Supervision, Writing - original draft, Writing - review & editing.

Acknowledgments

We are indebted to the patients and healthy volunteers for participating in this study. We acknowledge financial support by Land Schleswig-Holstein within the funding programme Open Access Publikationsfonds.

References

Alloway, K.D., Smith, J.B., Mowery, T.M., Watson, G.D.R., 2017. Sensory processing in the dorsolateral striatum: the contribution of thalamostriatal pathways. Front. Syst. Neurosci. 11 https://doi.org/10.3389/fnsys.2017.00053.

Avanzino, L., Tinazzi, M., Ionta, S., Fiorio, M., 2015. Sensory-motor integration in focal dystonia. Neuropsychologia 79, 288–300. https://doi.org/10.1016/j.neuropsychologia.2015.07.008.

Bara-Jimenez, W., Shelton;, P., Hallett, M., 2000a. Spatial discrimination is abnormal in focal hand dystonia. Neurology 55 (12), 1869–1873.

Bara-Jimenez, W., Shelton, P., Sanger, T.D., Hallett, M., 2000b. Sensory discrimination capabilities in patients with focal hand dystonia. Ann. Neurol. 47 (3), 377–380. https://doi.org/10.1002/(ISSN)1531-824910.1002/1531-8249(200003)47:3<>1.0.CO;2-110.1002/1531-8249(200003)47:3<377::AID-ANA16>3.0.CO;2-2.

Battistella, G., Termsarasab, P., Ramdhani, R.A., Fuertinger, S., Simonyan, K., 2017. Isolated focal dystonia as a disorder of large-scale functional networks. Cereb. Cortex bhv313. https://doi.org/10.1093/cercor/bhv313.

Berardelli, A., Conte, A., 2021. The use of botulinum toxin for treatment of the dystonias. Handb. Exp. Pharmacol. 263, 107–126. https://doi.org/10.1007/164_2019_339.

Bostan, A.C., Strick, P.L., 2018. The basal ganglia and the cerebellum: nodes in an integrated network. Nat. Rev. Neurosci. 19 (6), 338–350. https://doi.org/10.1038/s41583-018-0002-7.

Bradley, D., Whelan, R., Walsh, R., Reilly, R.B., Hutchinson, S., Molloy, F., Hutchinson, M., 2009. Temporal Discrimination Threshold: VBM evidence for an endophenotype in adult onset primary torsion dystonia. Brain 132 (9), 2327–2335. https://doi.org/10.1093/brain/awp156.

Bradnam, L.V., Graetz, L.J., McDonnell, M.N., Ridding, M.C., 2015. Anodal transcranial direct current stimulation to the cerebellum improves handwriting and cyclic drawing kinematics in focal hand dystonia. Front. Hum. Neurosci. 9 https://doi.org/10.3389/fnhum.2015.00286.

Caligiore, D., Pezzulo, G., Baldassarre, G., Bostan, A.C., Strick, P.L., Doya, K., Helmich, R. C., Dirkx, M., Houk, J., Jörntell, H., Lago-Rodriguez, A., Galea, J.M., Miall, R.C., Popa, T., Kishore, A., Verschure, P.F.M.J., Zucca, R., Herreros, I., 2017. Consensus paper: towards a systems-level view of cerebellar function: the interplay between cerebellum, basal ganglia, and cortex. The Cerebellum 16 (1), 203–229. https://doi.org/10.1007/s12311-016-0763-3.

Conte, A., Defazio, G., Hallett, M., Fabbrini, G., Berardelli, A., 2019. The role of sensory information in the pathophysiology of focal dystonias. Nat. Rev. Neurol. 15 (4), 224–233. https://doi.org/10.1038/s41582-019-0137-9.

Conte, A., McGovern, E.M., Narasimham, S., Beck, R., Killian, O., O'Riordan, S., Reilly, R. B., Hutchinson, M., 2017. Temporal discrimination: mechanisms and relevance to adult-onset dystonia. Front. Neurol. 8 https://doi.org/10.3389/fneur.2017.00625.

Conte, A., Rocchi, L., Ferrazzano, G., Leodori, G., Bologna, M., Li Voti, P., Nardella, A., Berardelli, A., 2014. Primary somatosensory cortical plasticity and tactile temporal discrimination in focal hand dystonia. Clin. Neurophysiol. 125 (3), 537–543. https://doi.org/10.1016/j.clinph.2013.08.006.

de Haan, E.H.F., Dijkerman, H.C., 2020. Somatosensation in the brain: a theoretical re-evaluation and a new model. Trends Cogn. Sci. 24 (7), 529–541.

Delmaire, C., Vidailhet, M., Elbaz, A., Bourdain, F., Bleton, J.P., Sangla, S., Meunier, S., Terrier, A., Lehericy, S., 2007. Structural abnormalities in the cerebellum and sensorimotor circuit in writer's cramp. Neurology 69 (4), 376–380. https://doi.org/10.1212/01.wnl.0000266591.49624.1a.

Delnooz, C.C.S., Helmich, R.C., Toni, I., van de Warrenburg, B.P.C., 2012. Reduced parietal connectivity with a premotor writing area in writer's cramp. Mov. Disord. 27 (11), 1425–1431. https://doi.org/10.1002/mds.25029.

Dresel, C., Li, Y., Wilzeck, V., Castrop, F., Zimmer, C., Haslinger, B., 2014. Multiple changes of functional connectivity between sensorimotor areas in focal hand dystonia. J. Neurol. Neurosurg. Psychiatry 85 (11), 1245–1252. https://doi.org/10.1136/jnnp-2013-307127.

Filip, P., Gallea, C., Lehéricy, S., Bertasi, E., Popa, T., Mareček, R., Lungu, O.V., Kašpárek, T., Vaníček, J., Bareš, M., 2017. Disruption in cerebellar and basal ganglia networks during a visuospatial task in cervical dystonia: Cerebellar Disruption in Cervical Dystonia. Mov. Disord. 32 (5), 757–768. https://doi.org/10.1002/mds.26930.

Fiorio, M., Tinazzi, M., Bertolasi, L., Aglioti, S.M., 2003. Temporal processing of visuotactile and tactile stimuli in writer's cramp. Ann. Neurol. 53 (5), 630–635. https://doi.org/10.1002/(ISSN)1531-824910.1002/ana.v53:510.1002/ana.10525.

Friston, K., 2009. Causal Modelling and Brain Connectivity in Functional Magnetic Resonance Imaging. PLoS Biol. 7 (2), e1000033. https://doi.org/10.1371/journal.pbio.1000033.10.1371/journal.pbio.1000033.g00110.1371/journal.pbio.1000033.g00210.1371/journal.pbio.1000033.g00310.1371/journal.pbio.1000033.t001.

Gallea, C., Herath, P., Voon, V., Lerner, A., Ostuni, J., Saad, Z., Thada, S., Solomon, J., Horovitz, S.G., Hallett, M., 2017. Loss of inhibition in sensorimotor networks in focal hand dystonia. Neuroimage Clin 13 (17), 90–97. https://doi.org/10.1016/j.nicl.2017.10.011.

Garraux, G., Bauer, A., Hanakawa, T., Wu, T., Kansaku, K., Hallett, M., 2004. Changes in brain anatomy in focal hand dystonia. Ann. Neurol. 55 (5), 736–739. https://doi.org/10.1002/(ISSN)1531-824910.1002/ana.v55:510.1002/ana.20113.

Ghaziri, J., Tucholka, A., Girard, G., Boucher, O., Houde, J.-C., Descoteaux, M., Obaid, S., Gilbert, G., Rouleau, I., Nguyen, D.K., 2018. Subcortical structural connectivity of insular subregions. Sci. Rep. 8 (1), 8596. https://doi.org/10.1038/s41598-018-26995-0.

Granert, O., Peller, M., Jabusch, H.-C., Altenmüller, E., Siebner, H.R., 2011. Sensorimotor skills and focal dystonia are linked to putaminal grey-matter volume in pianists. J. Neurol. Neurosurg. Psychiatry 82 (11), 1225–1231. https://doi.org/10.1136/jnnp.2011.245811.

Hanekamp, S., Simonyan, K., 2020. The large-scale structural connectome of task-specific focal dystonia. Hum. Brain Mapp. n/a(n/a) https://doi.org/10.1002/hbm.25012.

Kaji, R., Rothwell, J.C., Katayama, M., Ikeda, T., Kubori, T., Kohara, N., Mezaki, T., Shibasaki, H., Kimura, J., 1995. Tonic vibration reflex and muscle afferent block in writer's cramp. Ann. Neurol. 38 (2), 155–162. https://doi.org/10.1002/ana.v38:210.1002/ana.410380206.

Khosravani, S., Buchanan, J., Johnson, M.D., Konczak, J., 2020. Effect of neck botulinum neurotoxin injection on proprioception and somatosensory-motor cortical processing in cervical dystonia. Neurorehab. Neural Repair 34 (4), 309–320. https://doi.org/10.1177/1545968320905799.

Kitada, R., Hashimoto, T., Kochiyama, T., Kito, T., Okada, T., Matsumura, M., Lederman, S.J., Sadato, N., 2005. Tactile estimation of the roughness of gratings yields a graded response in the human brain: an fMRI study. NeuroImage 25 (1), 90–100. https://doi.org/10.1016/j.neuroimage.2004.11.026.

Lacruz, F., Artieda, J., Pastor, M.A., Obeso, J.A., 1991. The anatomical basis of somaesthetic temporal discrimination in humans. J. Neurol. Neurosurg. Psychiatry 54 (12), 1077–1081. https://doi.org/10.1136/jnnp.54.12.1077.

Lanciego, J.L., Luquin, N., Obeso, J.A., 2012. Functional Neuroanatomy of the Basal Ganglia. Cold Spring Harbor Perspect. Med. 2 (12), a009621. https://doi.org/10.1101/cshperspect.a009621.

Lehéricy, S., Ducros, M., Moortele, P.-F.-V.-D., Francois, C., Thivard, L., Poupon, C., Swindale, N., Ugurbil, K., Kim, D.-S., 2004. Diffusion tensor fiber tracking shows distinct corticostriatal circuits in humans. Ann. Neurol. 55 (4), 522–529. https://doi.org/10.1002/ana.20030.

Milardi, D., Quartarone, A., Bramanti, A., Anastasi, G., Bertino, S., Basile, G.A., Buonasera, P., Pilone, G., Celeste, G., Rizzo, G., Bruschetta, D., Cacciola, A., 2019. The cortico-basal ganglia-cerebellar network: past, present and future perspectives. Front. Syst. Neurosci. 13 https://doi.org/10.3389/fnsys.2019.00061.

Molloy, F.M., Carr, T.D., Zeuner, K.E., Dambrosia, J.M., Hallett, M., 2003. Abnormalities of spatial discrimination in focal and generalized dystonia. Brain 126 (10), 2175–2182. https://doi.org/10.1093/brain/awg219.

Moore, R.D., Gallea, C., Horovitz, S.G., Hallett, M., 2012. Individuated finger control in focal hand dystonia: an fMRI study. NeuroImage 61 (4), 823–831. https://doi.org/10.1016/j.neuroimage.2012.03.066.

Neychev, V.K., Gross, R.E., Lehéricy, S., Hess, E.J., Jinnah, H.A., 2011. The functional neuroanatomy of dystonia. Neurobiol. Dis. 42 (2), 185–201. https://doi.org/10.1016/j.nbd.2011.01.026.

Oldfield, R.C., 1971. The assessment and analysis of handedness: the Edinburgh inventory. Neuropsychologia 9 (1), 97–113.

Pastor, M.A., Day, B.L., Macaluso, E., Friston, K.J., Frackowiak, R.S.J., 2004. The functional neuroanatomy of temporal discrimination. J. Neurosci. 24 (10), 2585–2591. https://doi.org/10.1523/JNEUROSCI.4210-03.2004.

Pastor, M.A., Macaluso, E., Day, B.L., Frackowiak, R.S.J., 2008. Putaminal activity is related to perceptual certainty. NeuroImage 41 (1), 123–129. https://doi.org/10.1016/j.neuroimage.2008.01.034.

Peller, M., Zeuner, K.E., Munchau, A., Quartarone, A., Weiss, M., Knutzen, A., Hallett, M., Deuschl, G., Siebner, H.R., 2006. The basal ganglia are hyperactive during the discrimination of tactile stimuli in writer's cramp. Brain: A J. Neurol. 129, 2697–2708. https://doi.org/10.1093/brain/awl181.

Penny, W.D., Stephan, K.E., Daunizeau, J., Rosa, M.J., Friston, K.J., Schofield, T.M., Leff, A.P., Kording, K.P., 2010. Comparing families of dynamic causal models. PLoS Comput. Biol. 6 (3), e1000709. https://doi.org/10.1371/journal.pcbi.100070910.1371/journal.pcbi.1000709.g00110.1371/journal.pcbi.1000709.g00210.1371/journal.pcbi.1000709.g00310.1371/journal.pcbi.1000709.g00410.1371/journal.pcbi.1000709.g00510.1371/journal.pcbi.1000709.g00610.1371/journal.pcbi.1000709.g00710.1371/journal.pcbi.1000709.g00810.1371/journal.pcbi.1000709.t00110.1371/journal.pcbi.1000709.t00210.1371/journal.pcbi.1000709.s001.

Pool, E.-M., Rehme, A.K., Fink, G.R., Eickhoff, S.B., Grefkes, C., 2013. Network dynamics engaged in the modulation of motor behavior in healthy subjects. NeuroImage 82, 68–76. https://doi.org/10.1016/j.neuroimage.2013.05.123.

Preusser, S., Thiel, S.D., Rook, C., Roggenhofer, E., Kosatschek, A., Draganski, B., Blankenburg, F., Driver, J., Villringer, A., Pleger, B., 2015. The perception of touch and the ventral somatosensory pathway. Brain 138 (3), 540–548. https://doi.org/10.1093/brain/awu370.

Quartarone, A., Hallett, M., 2013. Emerging concepts in the physiological basis of dystonia. Mov. Disord. 28 (7), 958–967. https://doi.org/10.1002/mds.25532.

Ramnani, N., 2012. Frontal lobe and posterior parietal contributions to the cortico-cerebellar system. Cerebellum 11 (2), 366–383. https://doi.org/10.1007/s12311-011-0272-3.

Reig, R., Silberberg, G., 2014. Multisensory integration in the mouse striatum. Neuron 83 (5), 1200–1212. https://doi.org/10.1016/j.neuron.2014.07.033.

Rothkirch, I., Granert, O., Knutzen, A., Wolff, S., Gövert, F., Pedersen, A., Zeuner, K.E., Witt, K., 2018. Dynamic causal modeling revealed dysfunctional effective connectivity in both, the cortico-basal-ganglia and the cerebello-cortical motor network in writers' cramp. NeuroImage: Clin. 18, 149–159. https://doi.org/10.1016/j.nicl.2018.01.015.

Sanger, T.D., Tarsy, D., Pascual-Leone, A., 2001. Abnormalities of spatial and temporal sensory discrimination in writer's cramp. Mov. Disord. 16 (1), 94–99. https://doi.org/10.1002/(ISSN)1531-825710.1002/1531-8257(200101)16:1<>1.0.CO;2-F10.1002/1531-8257(200101)16:1<94::AID-MDS1020>3.0.CO;2-O.

Scontrini, A., Conte, A., Fabbrini, G., Colosimo, C., Di Stasio, F., Ferrazzano, G., Berardelli, A., 2011. Somatosensory temporal discrimination tested in patients receiving botulinum toxin injection for cervical dystonia. Movement Disord.: Off. J. Movement Disord. Soc. 26 (4), 742–746. https://doi.org/10.1002/mds.23447.

Simonyan, K., 2018. Neuroimaging Applications in Dystonia. In: International Review of Neurobiology (Bd. 143, S. 1–30). Elsevier. https://linkinghub.elsevier.com/retrieve/pii/S0074774218301077.

Stephan, K.E., Penny, W.D., Moran, R.J., den Ouden, H.E.M., Daunizeau, J., Friston, K.J., 2010. Ten simple rules for dynamic causal modeling. NeuroImage 49 (4), 3099–3109. https://doi.org/10.1016/j.neuroimage.2009.11.015.

Suttrup, I., Oberdiek, D., Suttrup, J., Osada, N., Evers, S., Marziniak, M., 2011. Loss of sensory function in patients with idiopathic hand dystonia. Mov. Disord. 26 (1), 107–113. https://doi.org/10.1002/mds.23425.

Trompetto, C., Currà, A., Buccolieri, A., Suppa, A., Abbruzzese, G., Berardelli, A., 2006. Botulinum toxin changes intrafusal feedback in dystonia: A study with the tonic vibration reflex. Mov. Disord. 21 (6), 777–782. https://doi.org/10.1002/mds.20801.

Tzvi, E., Stoldt, A., Witt, K., Krämer, U., 2015. Striatal–cerebellar networks mediate consolidation in a motor sequence learning task: an fMRI study using dynamic causal modelling. NeuroImage 122 (15), 52–64. 10.1016/j.neuroimage.2015.07.077.

Van Boven, R.W., Johnson, K.O., 1994. The limit of tactile spatial resolution in humans: grating orientation discrimination at the lip, tongue, and finger. Neurology 44 (12), 2361–2366. https://doi.org/10.1212/wnl.44.12.2361.

Walsh, R., Hutchinson, M., 2007. Molding the sensory cortex: Spatial acuity improves after botulinum toxin treatment for cervical dystonia. Mov. Disord. 22 (16), 2443–2446. https://doi.org/10.1002/mds.v22:1610.1002/mds.21759.

Wiestler, T., McGonigle, D.J., Diedrichsen, J., 2011. Integration of sensory and motor representations of single fingers in the human cerebellum. J. Neurophysiol. 105 (6), 3042–3053. https://doi.org/10.1152/jn.00106.2011.

Zeuner, K.E., Knutzen, A., Granert, O., Götz, J., Wolff, S., Jansen, O., Dressler, D., Hefter, H., Hallett, M., Deuschl, G., Eimeren, T., Witt, K., 2015. Increased volume and impaired function: the role of the basal ganglia in writer's cramp. Brain Behav. 5 (2) https://doi.org/10.1002/brb3.2015.5.issue-210.1002/brb3.301.